Experimental Investigation of Sonic Jet Flows
for Wing/Nacelle Integration

Eui-Yong Kwon*[†]

Powertrain Technology Lab., Institute for Advanced Engineering

Roger Leblanc, Jean-Henri Garem

*Laboratoire d'Etudes Aérodynamiques, Centre d'Etudes Aérodynamiques et Thermiques, 86036 Poitiers,
France*

An experimental study of compressible jet flows has been undertaken in a small transonic
wind tunnel. The aim of this investigation was to realize a jet simulator in the framework of
wing/nacelle integration research and to characterize the jet flow behavior. First, free jet
configuration, and subsequently jet flow in co-flowing air stream configuration were analyzed.
Flow conditions were those encountered in a typical flight condition of a generic transport
aircraft, i.e. fully expanded sonic jet flows interacting with a compressible external flowfield.
Conventional experimental techniques were used to investigate the jet flows-Schlieren visual-
ization and two-component Laser Doppler Velocimetry (LDV). The mean and fluctuating
properties were measured along the jet centerline and in the symmetric plane at various
downstream locations. The results of two configurations show remarkable differences in the
mean and fluctuating components and agree well with the trend observed by other investigators.
Moreover, these experiments enrich the database for such flow conditions and verify the
feasibility of its application in future aerodynamic research of wing/nacelle interactions.

Key Words : Free Jet, Co-Flowing Jet, Fully Expanded Sonic Jet Flow, Compressible Flow,
LDV

1. Introduction

The high bypass flow ratios of the advanced
power plants is associated with a growth in the
engine nacelle dimensions. Thus, the problem of
engine integration onto a wing has become more
important. Aerodynamic optimization of the en-
gine location is considered to be one of the key
factors that influence the overall flight perform-
ance. Consequently, the understanding of flow

[†] First Author

* Corresponding Author,
  E-mail : eykwon@iae.re.kr
  TEL : +82-31-330-7426; FAX : +82-31-33-7113
  Powertrain Technology Lab., Institute for Advanced
  Engineering, P.O. B.OX   25, 633-2 Koan-ri, paegam-
  myun, Yongin, Kyunggi-do 449-800, Korea.(Manusc-
  ript **Received** September 29, 2000; **Revised** January 8,
  2001)

interactions for aerodynamic optimization has
been the subject of a large number of
experimental (Godard et al., 1991, 1996, Rossow
et al., 1994) and numerical studies (Chaput et al. ,
1996, Rudnik et al. , 1996). To reduce develop-
ment cost and to obtain detailed data, feasibility
tests in an existing small wind tunnel were carried
out. As part of the research into improved
aerodynamic integration of nacelle under the
wing, an investigation of compressible jet flows
was undertaken in a small transonic wind tunnel
of the Centre d'Etudes Aérodynamiques et
Thermiques(CEAT) using a jet simulator. Within
the qualification tests required for wing/nacelle
integration applications, the implementation of
this model was subject to preliminary studies. The
objectives of the present investigation were to
characterize the jet flow behavior in quiescent and
co-flowing compressible stream, and especially to

prove that the quality of these jets can be satis-factory despite a complex air-handling problem related to the air jet drive system. This study examined the feasibility using models prior to complete wing/nacelle model testing. These experiments were conducted with an axisymmetric convergent nozzle, and the mean and fluctuating velocity components were measured.

The results presented here correspond to one of two flow condctions tested. For this case, the jet exit Mach number and the expansion ratio are close to unity, which lead to a fully expanded sonic jet flow. The external flow Mach number is chosen to be 0.79, which is close to cruise conditions.

2. Experimental Apparatus

Tests were conducted in the $150 \times 150 \times 1705mm^3$ test section of the transonic open-circuit wind tunnel at CEAT. It is capable of operating at stagnation pressures from 1 to 4 bar. Glass windows are installed in the sidewalls to measure and visualize the flowfield around the model. Tunnel conditions were fixed at an external flow Mach number of 0.79 and a Reynolds number, based on nozzle exit diameter, of 2.1×10^5. During the tests, the stagnation pressure p_{te} and the stagnation temperature T_{te} of the external stream and the jet flow were close to $1.3 \pm 0.05 \times 10^5 Pa$, $279 \pm 6K$ and $1.75 \times 10^5 Pa$, $269 \pm 3K$, respectively. At the nominal condition, the jet expansion ratio is fixed at $\gamma = p_j/p_e = 1$ with a compression ratio $(q = p_{tj}/p_e)$ value close to 1.9 to obtain a fully expanded jet flow. A summary of the flow conditions for this investigation is shown in Table 1.

The model used for simulating the jet flow is a 120 mm long cylindrical nacelle with a semi-ogive nose as shown in Fig. 1. It has an axisy-mmetric convergent nozzle with an exit diameter of 12 mm and a convergence angle of 10 deg. A pressure tap is located 2 mm ahead of the nozzle exit in order to measure local jet velocity. The nacelle is supported from the nose by a string-strut arrangement with its centerline on the sym-metric plane of the test section. The nacelle sup-
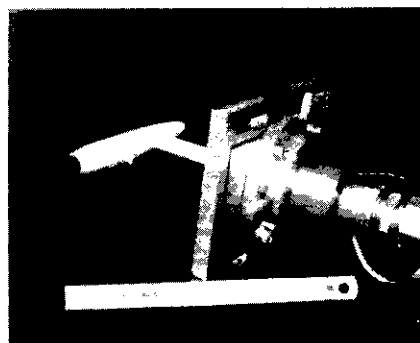

Fig. 1 Jet simulator

port strut is mounted perpendicularly in a vertical plane from the tunnel floor and its rig allows the axial and vertical positions to be varied in the useful range. Jet flow is carried out by the strut through the rig to provide an independently con-trolled coaxial jet stream. In general, the asymmetrical flow on the boattail caused by the strut interference, i.e. mixing in the wake down-stream of the strut, can produce pressure waves and blockage effects, which can be transmitted to the model, and hence affecting the jet plume behavior (Laughrey et Richey, 1976). The strut shape, dimension, and location were previously optimized; an aerodynamically improved strut profile was adopted in this study. The pressure upstream of the nozzle, p_x, and the static pressure at the exit, p_j, were controlled by a valve and measured by Bell&Howell 34.5 bar and 2 bar transducers, respectively. The maximum uncer-tainties for the present expansion ratio were less than 2%.

A conventional Schlieren device was employed to examine the flow field qualitatively. Continu-ous and spark Schlieren photographs were obtained with an exposure time of 4 ms and 4 μs, respectively. The wing pressure distribution is measured using a pressure scanning system with 48 port valves. This system is connected by tubing to a 2 bar transducer. Moreover, 2-D Laser Doppler Velocimetry (LDV) was used to measure the flow velocities.

A sketch of the test facility setup with the LDV system is shown in Fig. 2. The LDV system is comprised of a 10W Argon-ion laser of Spectra Physics operating on the green and blue lines with

Table 1 Flow parameters

Parameters	External flow		Jet
Mach number	0.79		1
Stagnation pressure, $p_t \times 10^{-5}$(Pa)	1.38		≈ 1.75
Static pressure, $p \times 10^{-5}$(Pa)	0.91		0.92
Stagnation temperature (K)	279 ± 6		269 ± 3
Velocity, V (ms^{-1})	249 ± 3		300 ± 2
Mass flow (kg.s^{-1})	7.2		45×10^{-3}
Reynolds, $Re_D \times 10^{-5}$(m^{-1})		2.1	
Expansion ratio, $r = p_j / p_e$		≈ 1	
Compression ratio, $q = p_{tj} / p_e$		≈ 1.9	
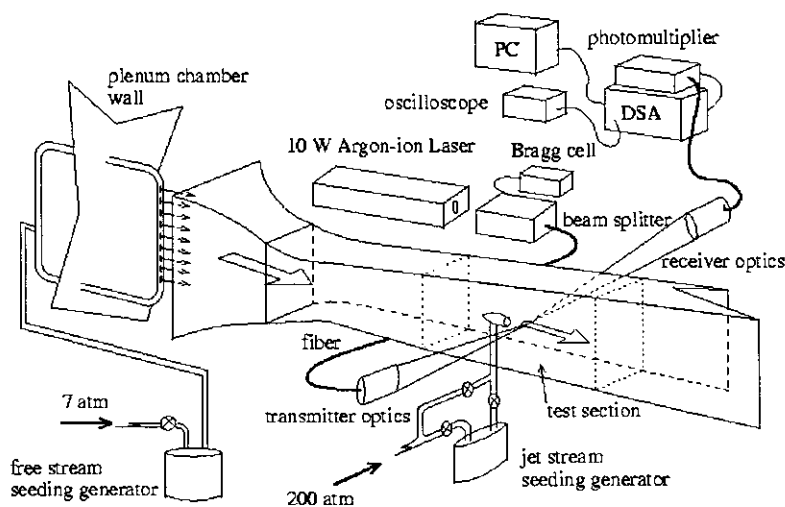
Fig. 2 Schematic of the LDV system

a wavelength and power of $0.5145\mu m$, 30mW and $0.488\mu m$, 45mW respectively. A 40 Mhz Bragg cell divided the laser beam into two beams of equal intensity and provided a frequency shift. A focusing lens created an interference fringe pattern and was connected to a system of photomultiplier, a "Doppler Signal Analyzer" (Model DSA 3000, Aerometrics), and a PC.

The signals from photomulipliers are processed to form ensemble averages from 3000 and 4000 individual velocities to obtain a converged mean and RMS values (the sampling rate in the present study was between 10 and 20 kHz). The probe volume is roughly cylindrical in shape with a length of approximately 1.5 mm and a diameter of 0.2 mm. The focal distance is 500 mm and the green and blue fringe spacing are 12.8 μm and 12.2 μm, respectively. The LDV optics operated in a
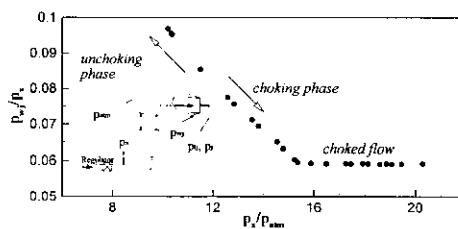
Fig. 3 Calibration of the fully expanded sonic jet flow

forward scatter mode and it is mounted on a three-axis, computer-controlled traversing mechanism supplied by DeltaLab. Thus, the probe volume was positioned to within ± 0.2 mm. The external stream is seeded through a movable tube placed in the plenum chamber, and the jet stream is seeded by a system of valves to control the particle mass flow rate (see Fig. 1). The seeding particles are
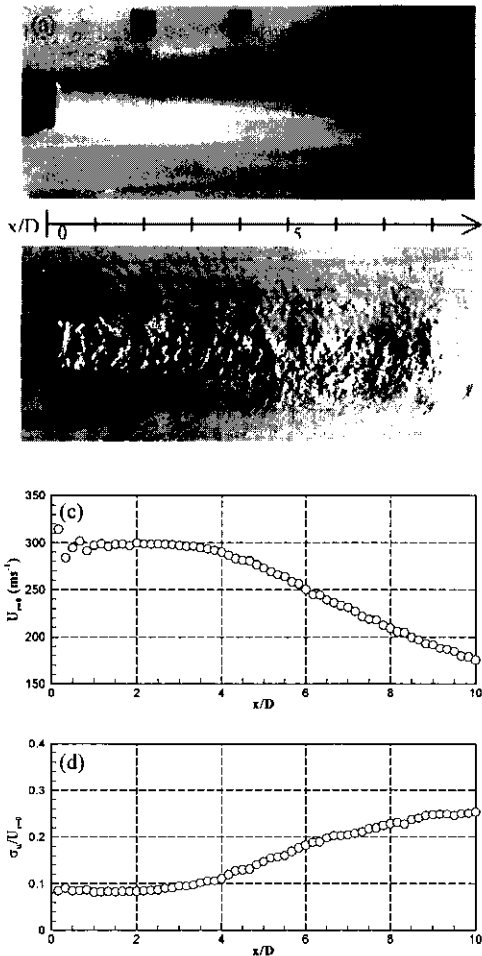
Fig. 4 Characteristics of the free jet flow, (a) continuous Shlieren photograph, (b) spark Shlieren photograph, (c) distributions of axial mean velocity, and (d) intensity of turbulence along the centerline of the free jet

submicronic (0.5 μm diameter) silica dioxide (SiO$_2$) of 2 gcm^{-3} volumetric mass, selected according to Bisschop (1993) and Lammari (1996). A brief review of diverse systematic biases met in compressible flows is given by Kwon (1999), in which the author estimates the uncertainty due to compressibility effects. For the present jet configuration, this uncertainty was found to be less than 2% for the external flow and 5% for the jet flow at the nozzle exit. This is consistent with the results of Nouri et al. (1996).

3. Results and Discussion

3.1 Calibration

Investigations of wing/jet interaction for various nacelle positions require a local pressure tap near the nozzle exit to independently control flow conditions ($M_j=1$, $r=p_j/p_e=1$). In fact, different positions of a nacelle relative to a wing correspond to different perturbation levels around the nozzle which may distort the real jet expansion ratio. This problem can be avoided by adjusting p_x until p_{wj} indicates sonic condition from the calibration data. The calibration is done in a free jet configuration, (i.e. jet exhausting into the atmosphere), by measuring simultaneously p_x, p_{wj} and p_j (with a static probe) or p_{tj} (with a Pitot tube). The details of calibration method and results are discussed in Kwon (1999). Figure 3 illustrates an example of calibration results, showing different phases of the jet flow. The jet Mach number is calculated from the pressure ratio of the calibration data by assuming constant total temperature, previously measured on the centerline near the nozzle exit.

3.2 Free jet experiments

The global characteristics of jet flows can be evaluated first from Schlieren visualizations. Figures 4(a) and 4(b) show the radial diffusion of the jet and its mixing regions with associated turbulent structures. The continuous and spark Schlieren photographs reveal a shock near the nozzle exit and the acoustic waves generated by large scale turbulent structures. Figures 4(c) and 4(d) skow the essential features of the subsonic turbulent jet flowfield. In a distance up to $x/D=$ 3.5, the axial mean velocity U is relatively uniform (300 ms^{-1}) and the axial turbulent intensity σ_u the (RMS of u') is nearly constant (8%). The potential core length is about 1-2 jet diameters less than the results obtained by Donaldson et al. (1976) and Lau et al. (1979), where the experiments were conducted under similar conditions (i.e. fully expanded sonic jet with an axisymmetric convergent nozzle). Hill and Jenkins (1976) showed that the potential core
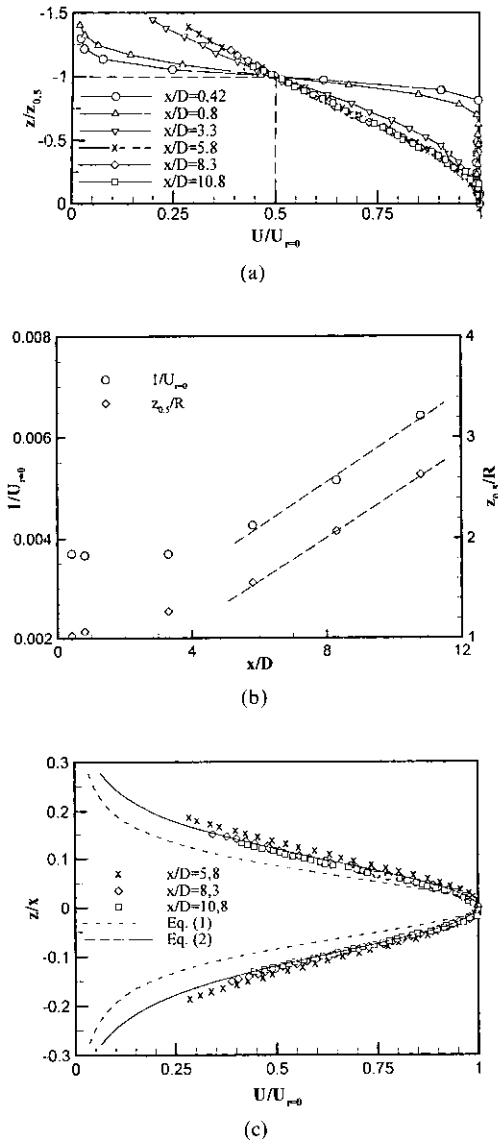
(a)

(b)

(c)

Fig. 5 Radial profiles of the turbulent quantities at various positions x/D; (a) axial and (b) radial intensities of turbulence and (c) turbulent shear stress

length as well as the flow structure depend strongly on the nature of initial boundary layer of the jet flow. In this configuration, the complex geometry of the jet flow handling system enhances turbulent flow and boundary layer development. Thus, axial velocity profile deviation can be generated at the nozzle exit. This may affect strongly the potential core length. In the nozzle

exit region, U oscillates spatially. This phenomenon, also shown by Mclaughlin et al. (1975) and Scroggs and Settles (1996), can be attributed to the effect of weak expansion waves occurring in this region.

In Fig. 5 the jet flow velocity data are presented. Figs 5(a) and (b) show the half width variations (i.e. $z_{0.5}$, the radial distance between the symmetric plane and the location of the half maximum mean velocity of the jet flow). The velocity profiles illustrate typical features of a subsonic jet. The potential core with constantly uniform value exists in the central region ($x/D<$ 3.3) and self-similar profiles exist in the developed region ($x/D\geq5.8$). The half widths and the inverse of centerline velocity measured on the symmetric plane $1/U_r=0$ increase linearly from $x/D=5.8$. With respect to these results, we estimate that the mean velocity field of the jet flow reaches self-preserving state, beyond $x/D=5.8$.

Figure 5(c) illustrates radial mean velocity distributions measured in the radial direction for three axial positions in the self-similar region, $x/D=5.8$, 8.3 and 10.8. As shown in the figure, the gradients are remarkably consistent and agree well with the existing semi-empirical curves. Here we compared the experimental data to the classical asymptotic profile proposed by Görtler and the equation defined by White (1991). These two equations are defined respectively as follows:

$$\frac{U}{U_{r=0}}=\left(1+\frac{\eta^2}{4}\right)^{-2}\text{with } \eta=15.2\frac{z}{x},$$

$$U_{r=0}\approx7.4\frac{\sqrt{J/\rho}}{x} \qquad (1)$$

where J is the jet momentum,

$$\frac{U}{U_{r=0}}=\sec h^2(\eta) \text{ with } \eta=\lambda\frac{z}{x} \qquad (2)$$

The proportional constant λ is experimentally determined to be 7.4. In general, λ is not universal and depends strongly on the nozzle geometry and upstream conditions (George, 1989). This dependency is observed in the experiments of Wygnanski et al. (1969) and Champagne et al. (1986).

Figure 6 illustrates the radial distributions of the two turbulence intensities, σ_u and σ_w, and the
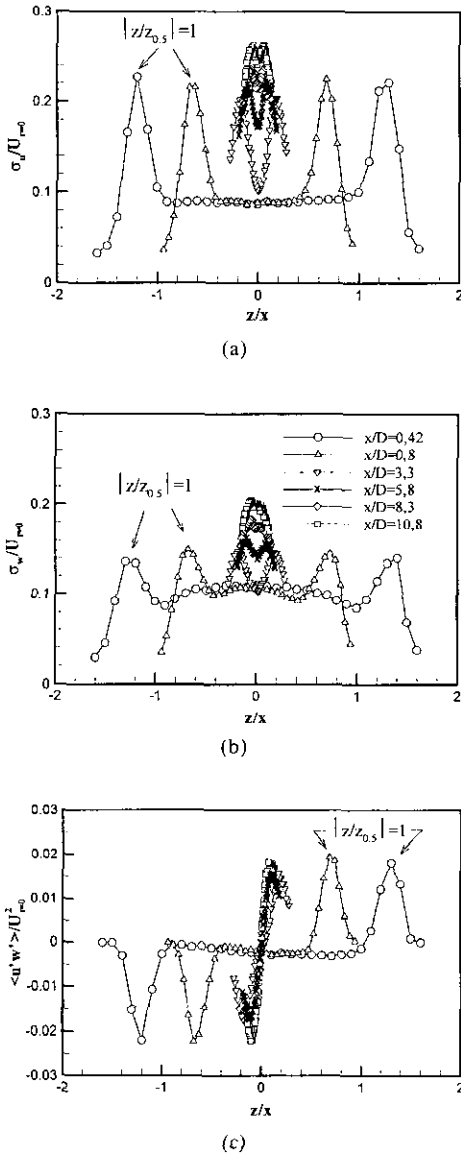
(a)

(b)

(c)

Fig. 6 Radial profiles of the turbulent quantities at various positions x/D; (a) axial and (b) radial intensities of turbulence and (c) turbulent shear stress
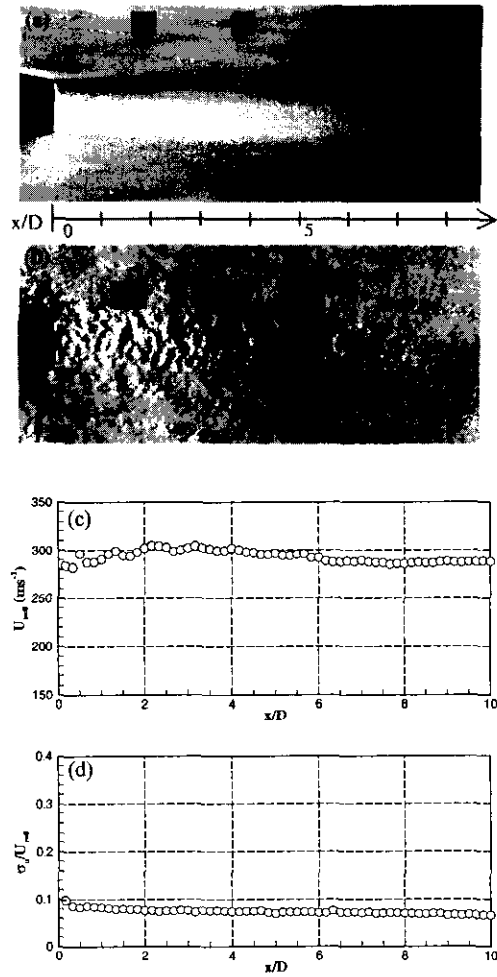

Fig. 7 Characteristics of the co-flowing jet; (a) continuous Shlieren photograph, (b) spark Shlieren photograph, distributions of axial (c) mean velocity, and (d) intensity of turbulence along the centerline of the free jet

turbulent shear stress $\langle u'w' \rangle$. All these quantities are normalized by the centerline jet velocity at the nozzle exit $U_{r=0}$. As expected, the intensities of turbulence take longer to develop than the axial mean velocity. This phenomenon is shown in the fully developed turbulent flow region where σ_u and σ_w don't become similar until $x/D=10.8$, unlike the mean velocity field. Generally, in this region, the highest turbulence intensity is observ-

ed in the centerline of the jet flow and decreases gradually with the radial distance. Here, the highest values of σ_u, σ_w and $\langle u'w' \rangle$ persist in the mixing region until $x/D=10.8$, and correspond to the half maximum mean velocity positions. The intensity of turbulence is relatively uniform in the central region of the jet flow with a maximum value of approximately 10%. At all measuring sections, σ_w is less than σ_u Thergore, the turbulence is anisotropic in the present jet flow.
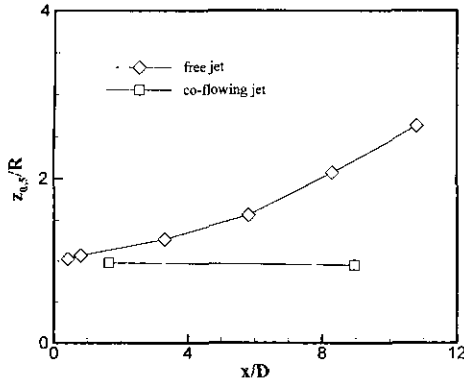
Fig. 8 Variations of half widths of the free and co-flowing jet flows

Fig. 9 Centerline variations of turbulent kinetic energy and shear stress

3.3 Co-flowing jet experiments

The general layout of the coaxial jet flow-field is given in Fig. 7 which shows the results of Schlieren visualizations and the axial distributions of U and σ_u. This figure shows the global effects of the co-flowing external stream in this configuration. In particular, the radial diffusion of the jet is less important than in the case of free jet flow. The sudden reduction of U, observed in free jet flow, is attenuated significantly due to the external flow and keeps a constant value close to 285 ms^{-1}, which is slightly higher than the external flow velocity (279 ms^{-1}). This difference (e.g. approximately 35% at $x/D=10$) doesn't allow identication of the potential core. A similar behavior was observed by Papamoschou (1997) in experiments with a co-annular nozzle at $M_j=$ 1.15, $M_\infty=0.75$. As shown in Fig. 7(d), σ_u decreases from 9% to 6.5% within 10 diameters. Unlike the free jet configuration, this turbulence intensity is relatively constant along the centerline at a value close to 0.075.

The jet flow development is also evaluated by analyzing the radial evolution of the half maximum velocity positions. As already observed from Schlieren photographs, external flow significantly reduces the radial development of the jet flow due to the increased entrainment rate, a well-known behavior of shear layers. Therefore, as seen in Fig. 8, the rate of growth of the half width is about one-twentieth of that of a free jet in a quiescent stream. In a distance between $x/D=0$
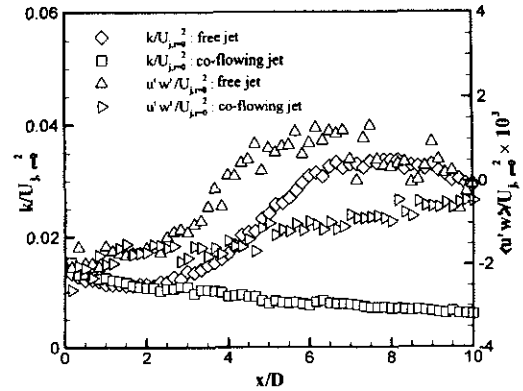
and 9, $z_{0.5}(x)$ is practically constant at a value close to R, whereas in the case of free jet, it increases nearly 100%. Thus, difference in turbulent fluctuations of the fluid particles exist between free and co-flowing jets. The slower growth rate of the half width of a jet in a co-flowing stream is consistent with the observations of Rho et al. (1993).

Figure 9 shows the centerline variations of turbulent kinetic energy k and turbulent shear stress $\langle u'w'\rangle$ for both configurations. These variables are normalized by the square of the centerline jet velocity. Since the velocity component v was not measured, k has been measured by the following formula, which was also used by Reijasse (1997):

$$k=0.5\left[\langle u'^2\rangle+\langle w'^2\rangle+0.5\left(\langle u'^2\rangle+\langle w'^2\rangle\right)\right] \quad (3)$$

In contrast to the free jet flow, k decays linearly with downstream position. The corresponding maximum value is 0.015 near the nozzle exit. The downstream increase in $\langle u'w'\rangle$, is smaller than that in a free jet flow due to the significant reduction of k resulting from the external flow.

4. Conclusions

Present experiments have allowed an investigation of the fully expanded sonic jet flow in a quiescent and co-flowing stream flow-field. The aim of this investigation was to realize a reliable jet simulator to study wing/nacelle integration

problem. The model test results were obtained with LDV.

The mean and fluctuating characteristics of the jet flows were generally in accordance with previous results particularly the characteristics of the potential and mixing region. In the case of co-flowing jet flow, the external stream reduced the diffusion rate of the mixing flow half widths and produced a uniform centerline mean and fluctuating velocity. Finally, these experiments demonstrated the feasibility of the present jet simulator in conducting a study of interactions on a complete wing/jet interaction model in this wind tunnel.

Acknowledgements

References

Bisschop, J. -R., 1993, "Comportement de la Turbulence en Couche de Mélange Supersonique," Ph. D. Thesis, CEAT-LEA, University of Poitiers, Poitiers.

Chaput, E., Gacherieu, C., and Tourrette, L., 1996, "Application of Navier-Stokes Methods for Engine/Airframe Integration," *Aspects of Engine-Airframe Integration for Transport Aircraft*, DLR Workshop Braunschweig, pp. 7/1~7/12.

Donaldson, C.D., and Snedecker, R.S., 1971, "A Study of Free Jet Impingement. Part 1. Mean Properties of Free and Impinging Jets," *J. Fluid Mechanics*, Vol. 45, Part. 2, pp. 281~319.

George, W.K., 1989, "The Self-Preservation of Turbulent Flows and its Relation to Initial Conditions and Coherent Structures," W. K George and R. Arndt (ed.), Advances in Turbulence, Hemisphere, New York, pp. 39~73.

Godard, J.L., Jacquotte, O.P., and Gisquet, D., 1991, "Analyse Detaillee de l'interaction voilure -nacelle d'un avion de transport civil," AGARD CP-498, *Aerodynamic Engine/Airframe Integra-*

tion for High Performance Aircraft and Missiles, FDP Symposium, Texas.

Godard, J.L., Hoheisel, H., Rossow, C.-C., and Schmitt, V., 1996, "Investigation of Interference Effects for Different Engine Positions on a Transport Aircraft Configuration," *Aspects of Engine-Airframe Integration for Transport Aircraft*, DLR Workshop Braunschweig, pp. 11/1 ~11/18.

Kwon, E.Y., 1999., "Contribution a l'Étude des Interactions Entre un Jet Sonique et un Écoulement Compressible Autour d'une Aile," Ph. D. Thesis, CEAT-LEA, University of Poitiers, Poitiers.

Lammari, M.R., 1996, "Mesures par Vélocimetrie Laser Doppler dans une Couche de Mélange Turbulente Supersonique : Quelques Aspects du Processus de Mesure," Ph. D. Thesis, CEAT-LEA, University of Poitiers, Poitiers.

Lau, J.C., Morris, P.J., and Fisher, M.J., 1979, "Measurements in Subsonic and Supersonic Free Jets using a Laser Velocimeter," *J. Fluid Mechanics*, Vol. 93, Part1, pp. 1~27.

Laughrey, J.A., Richey, G.K., 1976, "Data Variance due to Different Testing Techniques," AGARDograph No. 208, *Improved Nozzle Testing Techniques in Transonic Flow*, Part II, pp. -E1~E21.

McLaughlin, D.K., Morrison, G.L., and Troutt, T.R., 1975, "Experiments on the Instability Waves in a Supersonic Jet and Their Acoustic Radiations," *J. Fluid Mechanics*, Vol. 69, pp. 73 ~95.

Nouri, J.M., Whitelaw, J.H., 1996, "Flow Characteristics of an Underexpanded Jet and its Application to the Study of Droplet Breakup," *Exp. in Fluids*, Vol. 21, No. 10, pp. 243~247.

Papamoschou, D., 1997, "Mach Wave Elimination in Supersonic Jets," *AIAA Journal*, Vol. 35, No. 10, pp. 1604~1611.

Reijasse, P., and Corbel, B., 1997, "Expérience de Base sur les Phénomènes de Non-adaptation dans les Tuyères Aérospike," ONERA TP 1997 ~74.

Rho, B.J., Kang, S.J, and Oh, J.H., 1993, "LDV Measurements of Turbulence Characteristics in a Two Phase Coaxial Jet," *Proceeding of the 2nd*

Inter. Symp. on Enginneering Turbulence Modelling and Measurements, Engineering Turbulence Modelling and Experiments 2, pp. 437 ~446.

Rossow, C.-C., Godard, J.L., Hoheisel, H., and Schmitt, V., 1994, "Investigations of Propulsion Integration Interference Effects on a Transport Aircraft Configuration," *Journal of Aircraft*, Vol. 31, No. 5, pp. 1022~1030.

Rudnik, R., Ronzheimer, A., Schenk, M., and Rossow, C.-C., 1996, "Investigation of Interference Effects for Different Engine Positions on a Transport Aircraft Configuration," *Aspects of Engine-Airframe Integration for Transport Aircraft*, DLR Workshop Braunschweig, pp. 11/1 ~11/18.

Scroggs, S.D., and Settles, G.S., 1996, "An Experimental Study of Supersonic Microjets," *Exp. in Fluids*, Vol. 21, pp. 401~409.

White, F.M., 1991, *Visous Fluid Flow*, McGraw-Hill, 2nd Edition, p. 474.

Wignanski, I., and Fiedler, H., 1969, "Some Measurements in the Self-Preserving Jet," *J. Fluid Mechanics*, Vol. 38, Part 3, pp. 577~612.